

Electronic Supplementary Material (ESI) for Journal of Materials Chemistry A

This journal is © The Royal Society of Chemistry 2017

Litchi-like porous Fe/N/C spheres with atomically dispersed FeN_x promoted by sulfur as high-efficient oxygen electrocatalysts for Zn–air batteries

Qiliang Wei,[†] Gaixia Zhang,^{,†} Xiaohua Yang,[†] Yanqing Fu,[†] Guanhua Yang,[†] Ning Chen,[‡]
Weifeng Chen,[‡] Shuhui Sun^{*,†}*

[†]Institut National de la Recherche Scientifique-Énergie Matériaux et Télécommunications,
Varennnes, QC J3X 1S2, Canada.

[‡]Canadian Light Source (CLS), 44 Innovation Boulevard, Saskatoon, SK, S7N 2V3, Canada

Experimental Section

Materials

Phenol (99 %), formaldehyde solution (37 %), iron (II) acetate (95 %), 1,10 phenanthroline (99 %), sodium hydroxide (NaOH, 95.0 %), sulfur (S), and potassium hydroxide (KOH, 87.1 %), were bought from Fisher Scientific; Pluronic®F-127, Nafion solution (5 wt%) were purchased from Sigma-Aldrich. Pt/C (20%) was purchased from E-TEK. All chemicals were used as received and solutions were prepared using deionized water (Millipore Milli-Q, 18.2 MΩ cm).

Preparation of spherical phenolic resol-F127 monomicelles (SPRMs)^[1]

Firstly, F127 (0.96 g) was dissolved in 15 mL DI water at room temperature with stirring for 30 min. Then phenol (0.6 g), formaldehyde solution (2.1 mL), and NaOH aqueous solution (0.1 M, 15 mL) were mixed and stirred at 70 °C for 30 min to obtain a low-molecular-weight phenolic resols. After that, the F127 solution was dropped into the phenolic resols slowly with stirring. After 2 hrs, 50 mL of water was added and further stirred at 70 °C for 12-14 hrs. Afterwards, 12 mL of the as-prepared monomicelle solution and 25 mL of H₂O was transferred into an autoclave (50 mL volume) for hydrothermal treatment at 130 °C for 20 hrs. In the end, the SPRMs were collected by centrifugation and washed with distilled water for several times, followed by a drying process in an oven at 60 °C, and then served as the carbon host for loading Fe and N in the next step.

Preparation of Fe/N/C catalysts

In a typical synthesis of S treated Fe/N/C catalyst, the precursors were prepared by first mixing 0.7 g SPRMs, 0.7 g S, 136 mg 1,10-Phen, 30 mg FeAc in a solution of ethanol

and deionized water (ethanol:water = 1:2) under stirring at room temperature. Then the mixture was heated to 60–80 °C for 2–3 hrs until about 30 ml of a thick slurry was obtained. The slurry was placed overnight in a drying oven at 95 °C. Afterwards, the dry powder was ground sufficiently and placed in the quartz tube, followed by heating at 450 °C in Ar for 2 hrs, and then pyrolyzed in Ar at 700 °C for 1 hr, followed by another pyrolysis in ammonia at 950 °C with different pyrolysis time in order to obtain expected ~50% weight remaining.^[2-5] In the experiment, different amount of S were used (the mass ratio of SPRMs/S = 0.5, 1.0, 1.5) to find the optimal S content of the S treated-Fe/N/C catalysts. For comparing, the porous Fe/N/C without the addition of S (denoted as untreated Fe/N/C) was prepared as the same process.

Physical characterizations

The morphological structures of the catalysts were investigated by transmission electron microscopy (TEM) and high-resolution TEM (HRTEM) (JEOL JEM-2100F, operated at 200 kV). The surface properties were analysed by X-Ray photoelectron spectroscopy (XPS, VG ESCALAB 220i-XL) equipped with a hemispherical analyser for a Twin Anode X-Ray Source (Al K α was used in this work). The C 1s peak (BE = 284.6 eV) was used as the reference line to accurately determine the positions of other spectral lines. The fine structure of the photoelectron lines was treated using Casa XPS software (2.3.15 Version). The surface areas of the catalysts were measured through N₂ sorption isotherms that were collected using Quantachrome Instruments Autosorb-1 at liquid nitrogen temperature (77.3 K). The surface areas were estimated from the Brunauer-Emmett-Teller (BET) equation and from the fitting of the N₂-adsorption isotherms based on a slit-pore model, with the Quenched solid density functional theory (QSDFT) available in the AS1WIN software. The P/P₀ range is 0.05-0.35. QSDFT is the

most advanced DFT method developed from 2006 for the pore size analysis of geometrically and chemically disordered micro-mesoporous carbons, which allows the calculation of pore size distributions from ca. 0.6 nm up to ca. 40 nm. It allows for a major improvement of the accuracy of DFT pore size distribution analyses of disordered carbon materials from low-temperature nitrogen adsorption isotherms because it takes into account the effects of surface roughness, anisotropy and heterogeneity explicitly.

The Fe K-edge X-ray absorption near-edge structure (XANES) and Extended X-ray Absorption Fine Structure (EXAFS) data were collected on the 06ID-1 Hard X-ray MicroAnalysis (HXMA) beamline at the Canadian Light Source. During data collection, the CLS storage ring (2.9 GeV) was operated under 250 mA mode and the HXMA superconducting wiggler was run at 1.9 T. Measurements were made at room temperature in fluorescence mode using a 32-element Ge detector. Data collection configuration was using metal Fe foil as energy calibration by in step calibration for every data sets. To prepare the electrode for the XANES measurement, powder Fe/N/C catalysts were mixed with Nafion solution (5 wt%) and isopropanol to form homogeneous ink followed by dropping onto a gas diffusion layer (GDL). The spectra were normalized with respect to the edge height after subtracting the pre-edge and post-edge backgrounds, then convert the data from energy space to k space using Athena software.

Electrochemical measurements

All electrochemical measurements were carried out in a three-electrode cell using a rotating ring disk electrode (RRDE, PINE Research Instrumentation) with a bipotentiostat (Pine, Model PGSTAT-72637) workstation at room temperature. A Pt wire and a Hg/HgO were used as the counter and reference electrodes, respectively. All potentials in this study refer to reversible hydrogen electrode (RHE). A RDE with glassy carbon (GC) disk electrode (5 mm in diameter)

and a rotating ring-disk electrode (RRDE) with a Pt ring and a GC disk (5.61 mm diameter) were used as the substrate for the working electrodes. Before use, the GC electrodes in RDE/RRDE were polished using aqueous alumina suspension on felt polishing pads.

The catalyst suspension in this work was prepared as the following: 10 mg of catalyst was mixed in a glass vial with 95 μl of 5 wt% Nafion solution and 350 μl of ethanol, followed by sonication and agitation in a vortex mixer, alternatively, for a total of 1 h. Then 9 μl of the catalyst suspension was dropped onto the GC electrode surface ($\sim 0.8 \text{ mg cm}^{-2}$). For comparison, the 20 wt% Pt/C catalyst (E-ETK) was prepared with a loading amount of $100 \mu\text{g cm}^{-2}$ (i.e., $20 \mu\text{g}_{\text{Pt}} \text{ cm}^{-2}$). Before testing, N_2 (or O_2) was bubbled through the electrolyte for 30 min and the N_2 - (or O_2 -) was kept bubbling during the measurements, in order to keep the N_2 - or O_2 -saturated in the solution. In 0.1 M KOH, the cyclic voltammetry (CV) profiles were recorded at 50 mV s^{-1} and the linear sweep voltammograms (LSV) were recorded at 10 mV s^{-1} , between 0-1.2 V (vs. RHE). All of the LSV curves were recorded after subtraction of the background current recorded in N_2 -saturated solution. For detecting peroxide formed at the disc electrode, the potential for the Pt ring electrode was set at 1.3 V (vs. RHE) and the voltammograms were recorded at 1600 rpm. The collection efficiency of the ring-disk electrode was $N = 0.37$. The peroxide yield (H_2O_2 , %) and the electron transfer number (n) were calculated as follows:

$$\text{H}_2\text{O}_2\% = 200 \times (\text{I}_r/\text{N})/(\text{I}_d + \text{I}_r/\text{N})$$

$$n = 4 \times \text{I}_d / (\text{I}_d + \text{I}_r/\text{N})$$

Where I_d is the disk current and I_r is the ring current.

The stability of the catalysts was tested on fresh electrodes by chronoamperometry at 0.7 V (vs. RHE) for 500 min in O_2 -saturated 0.1 M KOH with a rotation speed of 1600 rpm.

Linear sweep voltammograms for the OER are obtained using a RDE (1600 rpm) in 1 M KOH solution at a scan rate of 10 mV s⁻¹ in O₂-saturated solution.

Zn-air battery assembly and measurement:

The Zn-air batteries were tested in home-built electrochemical cells, the electrolyte used was 6 M KOH and 0.2 M Zn(Ac)₂ solution. To prepare the air electrode, homogeneous catalyst ink consisting of Fe/N/C catalysts, Nafion solution (5 wt%) and isopropanol was dropped onto a gas diffusion layer (GDL) with a catalyst loading of ~1.0 mg cm⁻², a polished zinc plate was used as the anode. For comparing, 20 wt% Pt/C catalysts were prepared as the same procedure to achieve the same loading. Polarization data was collected using galvanodynamic method at a scan rate of 1.0 mA s⁻¹ with cut-off voltage of 0.6 V for the discharge and 2.2 V for the charge. Galvanostatic discharge and charge cycling was conducted at a constant current density of 5 mA cm⁻² with each cycle for 20 min.

Figures:

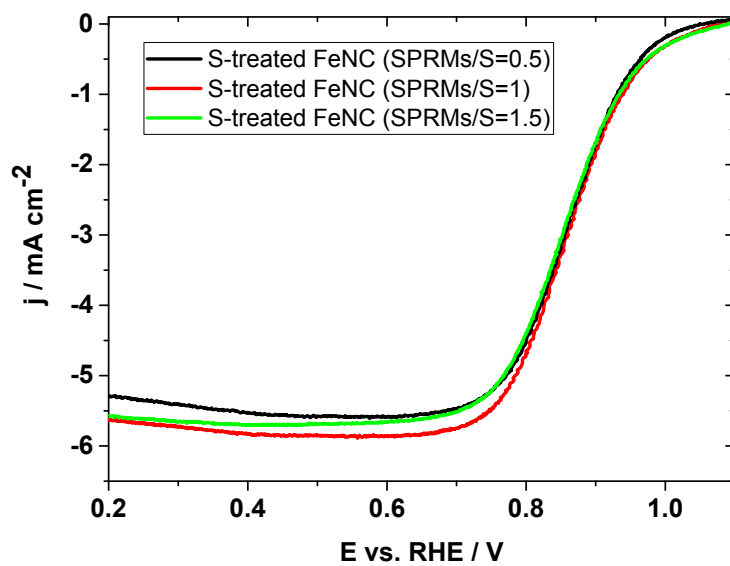


Figure S1. LSV results of (a) the S-treated Fe/N/C with different SPRMs/S ratio (scan rate = 10 mV s^{-1} , rotation rate = 1600 rpm).

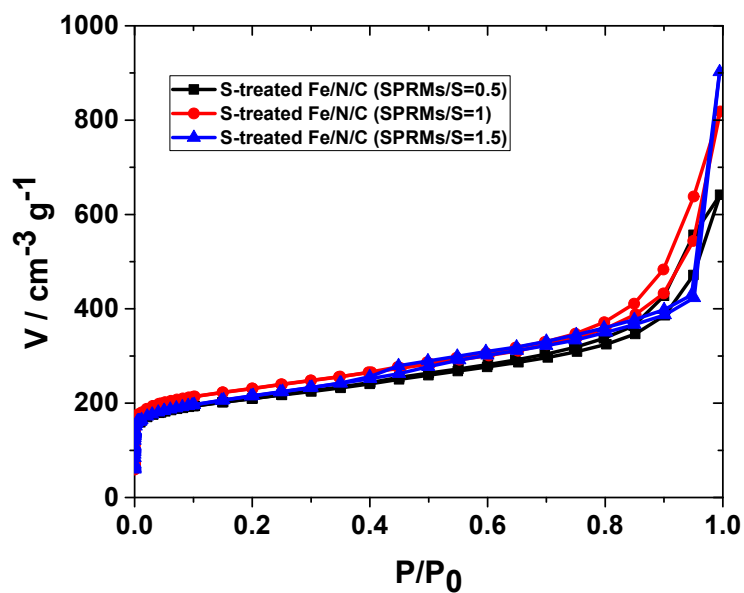


Figure S2. (a) N_2 adsorption/desorption of S-treated Fe/N/C samples.

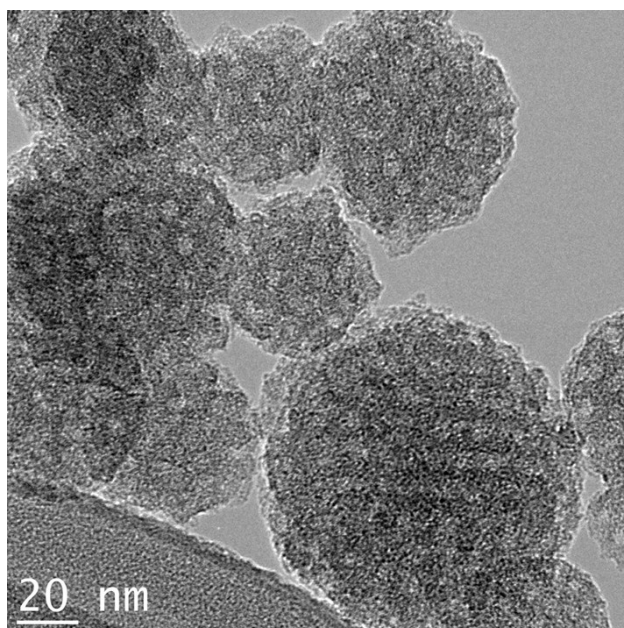


Figure S3. TEM image of S-treated Fe/N/C after Ar pyrolysis (before NH_3 pyrolysis).

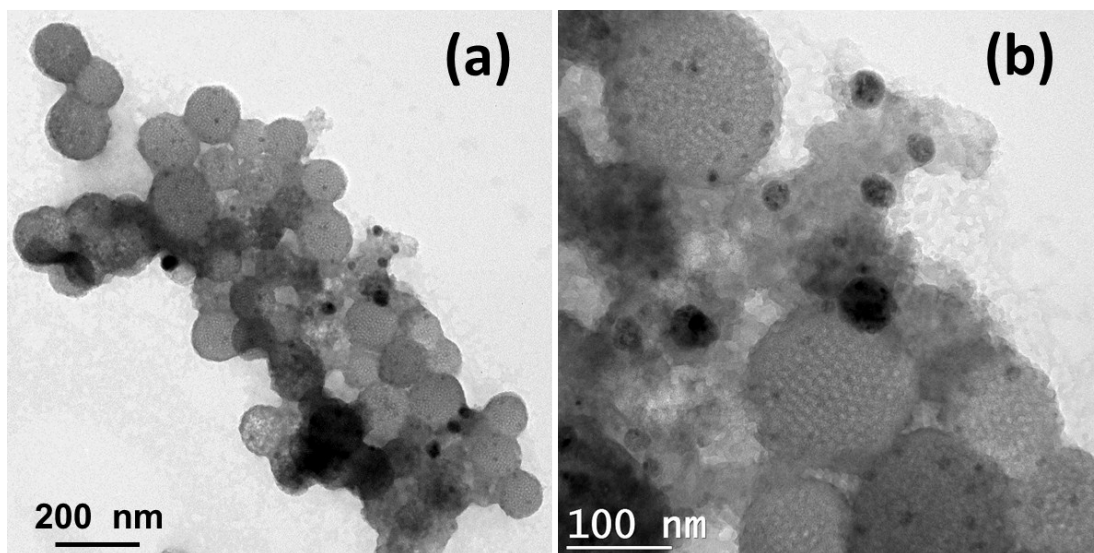


Figure S4. TEM images of S-treated Fe/N/C after NH_3 pyrolysis (S : SPRMs = 0.5)

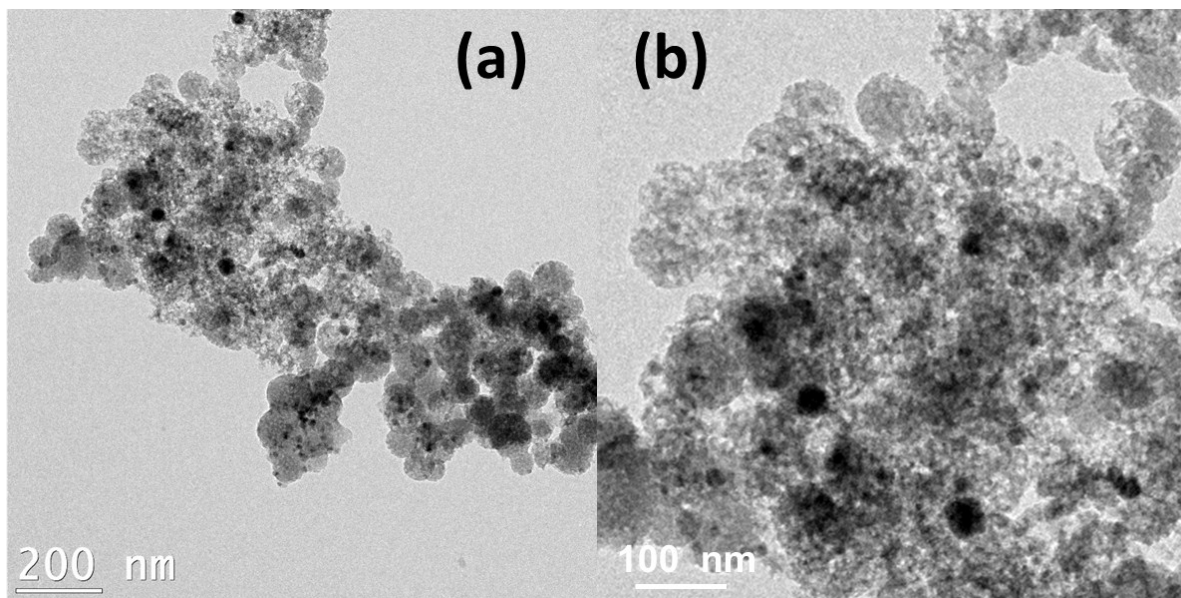


Figure S5. TEM images of S-treated Fe/N/C after NH₃ pyrolysis (S : SPRMs = 1.5)

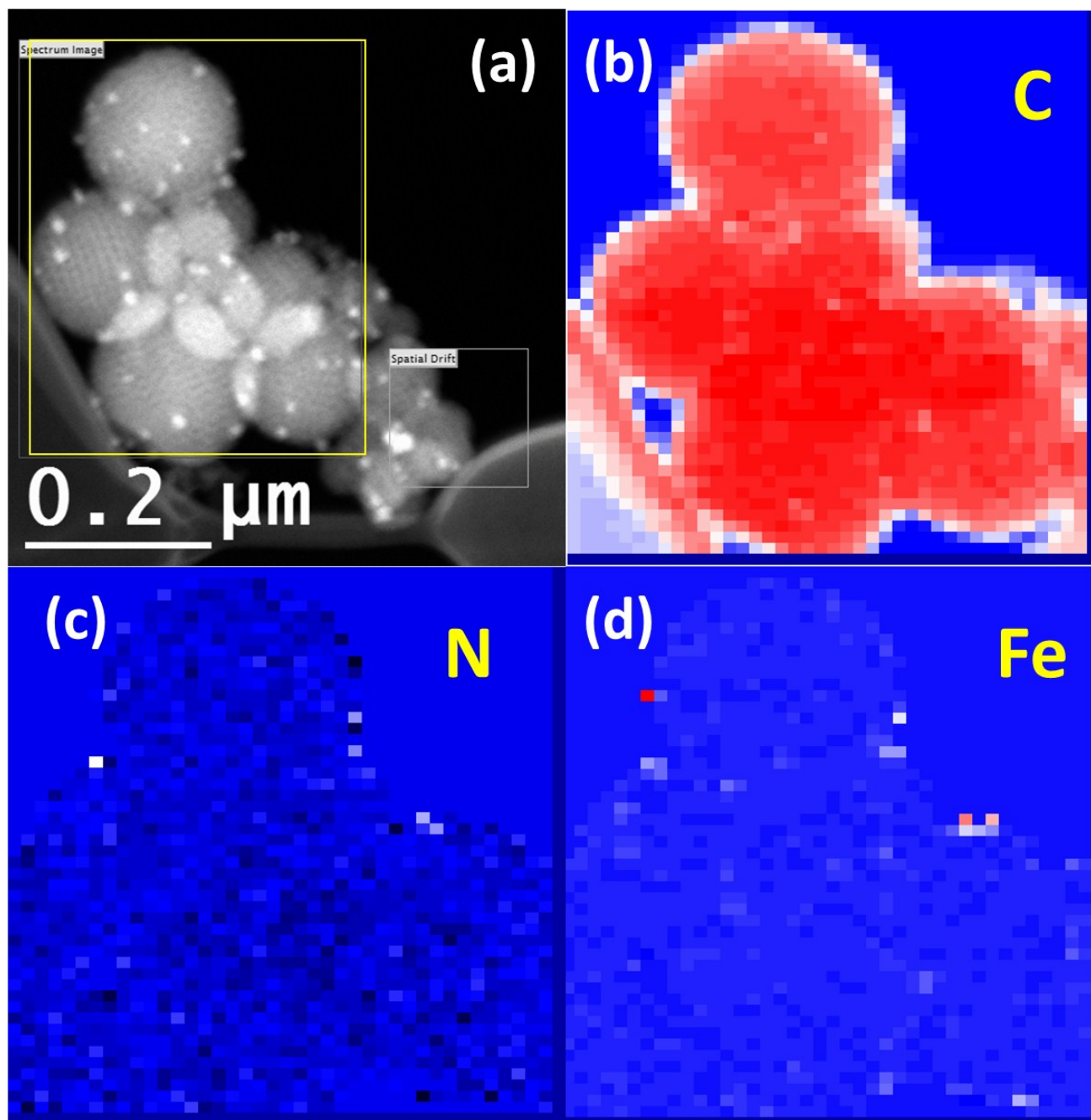


Figure S6. (a) HAADF TEM image, and (b-d) EELS mapping of C, N, and Fe of the area marked by yellow square in (a).

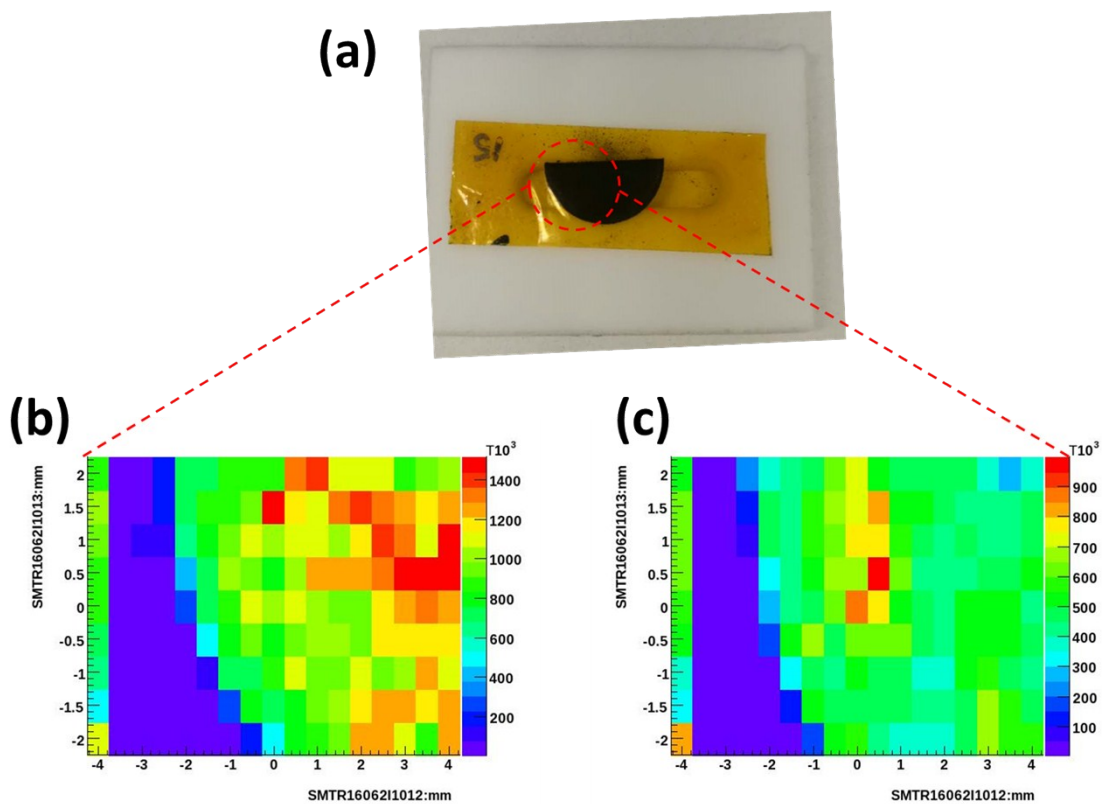


Figure S7. The 2D fluorescence mapping collected at 50 eV above the Fe K edge: (a) is the picture of the sample loaded on the holder, (b) Untreated Fe/N/C electrode, (c) S-treated Fe/N/C electrode.

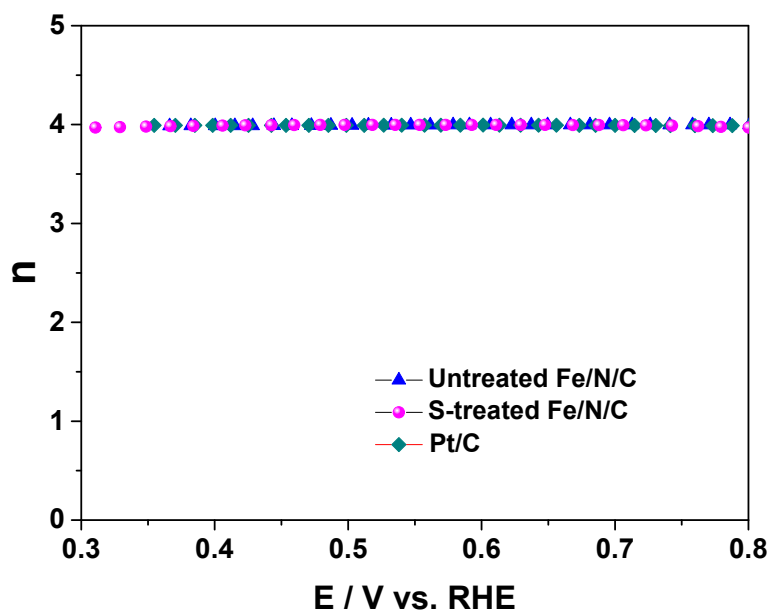


Figure S8. Electron-transfer numbers (n) of untreated Fe/N/C, S-treated Fe/N/C and Pt/C in O₂-saturated 0.1 M KOH at a scan rate of 10 mV s⁻¹, rotation rate = 1600 rpm.

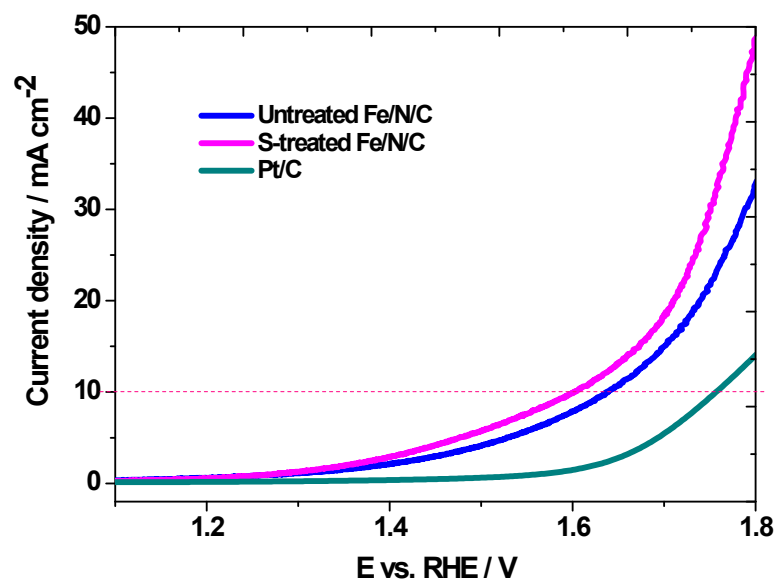


Figure S9. OER LSVs of untreated Fe/N/C, S-treated Fe/N/C, and Pt/C samples in 1 M KOH (scan rate = 10 mV s⁻¹, rotation rate = 1600 rpm).

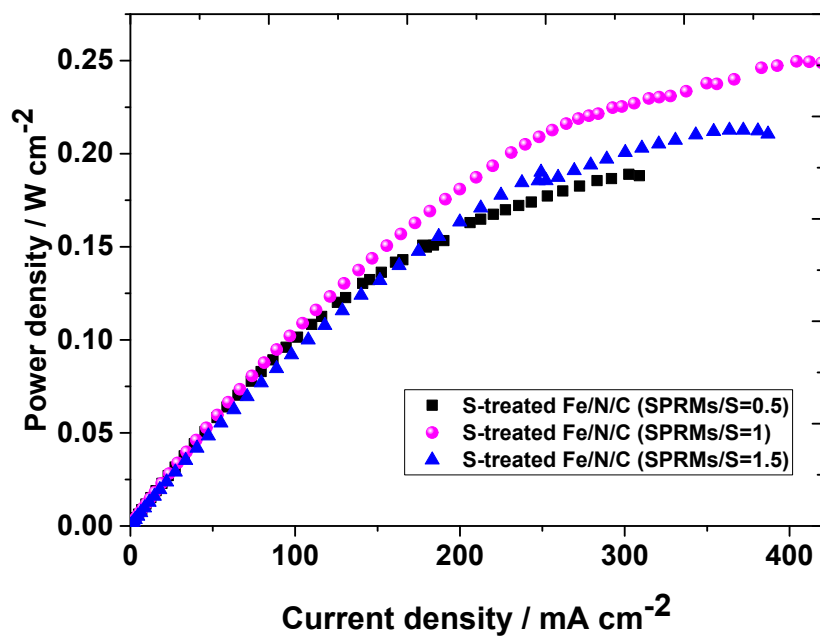


Figure S10. Power density of S-treated Fe/N/C samples, loading is ~ 1.0 mg cm⁻².

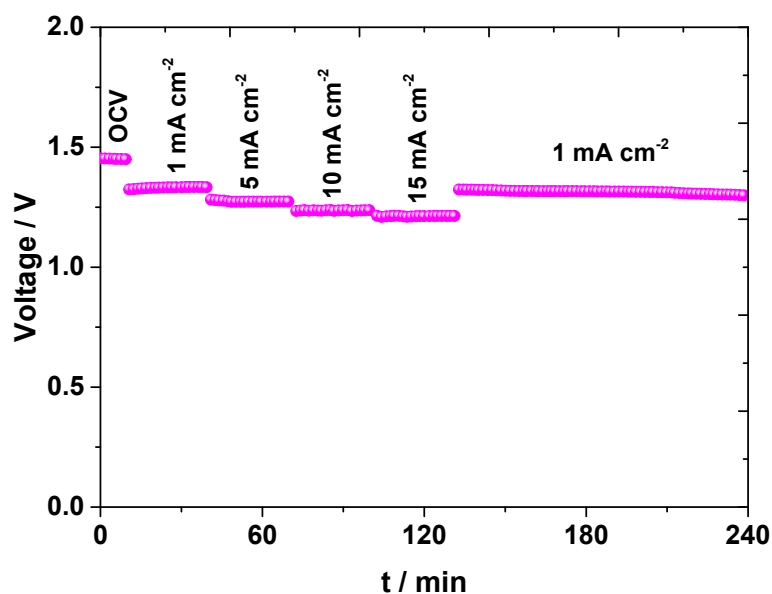


Figure S11. Discharge voltage of S-treated Fe/N/C sample at various current densities.

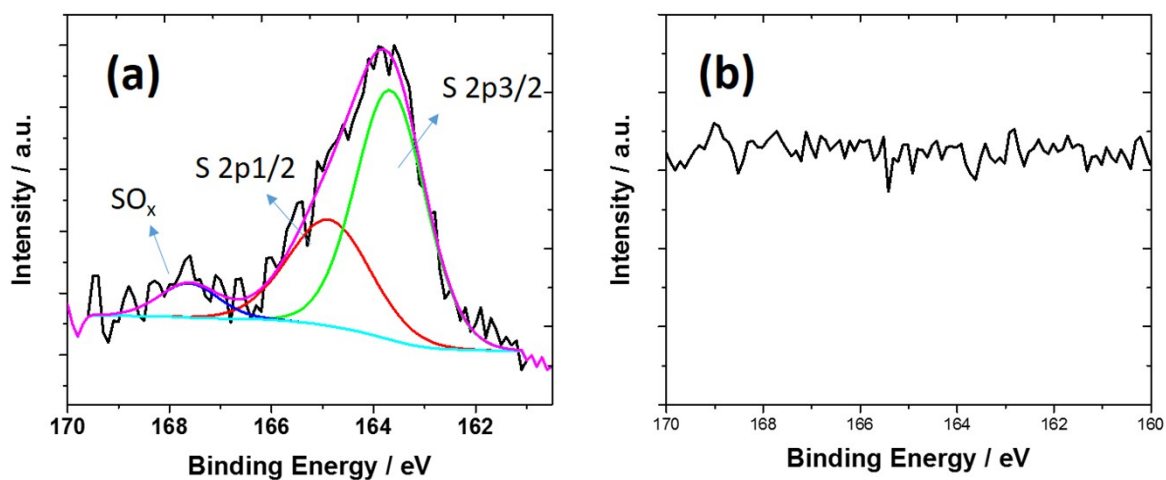


Figure S12. High-resolution of S 2p spectrum of S-treated Fe/N/C sample before (a) and after (b) NH_3 pyrolysis.

Table S1. N₂ adsorption/desorption parameters.

Samples	N ₂ adsorption/desorption			
	Surface area (m ² /g)	Surface area of micropore (m ² /g)	Surface area of mesopore (m ² /g)	Pore volume (cc/g)
Untreated Fe/N/C	536.3	435.7	100.6	0.586
S-treated Fe/N/C (SPRMs/S=0.5)	911.6	755.9	155.7	0.821
S-treated Fe/N/C (SPRMs/S=1)	982.1	810.1	172.0	1.01
S-treated Fe/N/C (SPRMs/S=1.5)	921.9	752.1	169.8	0.858

Table S2. Electrochemical performance comparison of zinc-air batteries employing various ORR catalysts as the cathode.

ORR Catalyst	Zn electrode	Electrolyte	Catalyst loading (mg cm ⁻²)	Cathode active material	Peak power density (mW cm ⁻²)	Ref.
Fe@N-C-700	Zn plate	6 M KOH + 0.2 M Zn(Ac) ₂	2.2	Air	220	S1 ^[6]
NiFe@NCX	Zn plate	6 M KOH	1.0	Air	~85	S2 ^[7]
Nitrogen-doped hierarchically porous carbon	Zn foil	6 M KOH	1.0	Air	80	S3 ^[8]
Co ₄ N/CNW/CC	Zn plate	6 M KOH + 0.2 M Zn(Ac) ₂	1.0	Air	174	S4 ^[9]
Co-doped TiO ₂ nanoparticle	Zn plate	6 M KOH + 0.2 M Zn(Ac) ₂	-	Air	136	S5 ^[10]
Fe-N-SCCFs	Zn foil	6 M KOH	1.0	O ₂	~300	S6 ^[11]
S ₃ N-Fe/N/C-CNT	Zn plate	6 M KOH + 0.2 M Zn(Ac) ₂	1.25	Air	102.7	S7 ^[12]
NiCo ₂ S ₄ /N-CNT	Zn foil	6 M KOH + 0.2 M ZnCl ₂	1.0	O ₂	147	S8 ^[13]

Carbon-Coated Core–Shell Fe–Cu Nanoparticles	Zn plate	6 M KOH	---	Air	212	S9 ^[14]
Co/CoO nanoparticles immobilized on Co–N-doped carbon	Zn foil	6 M KOH + 0.2 M ZnCl ₂	2.0	Air	157	S10 ^[15]
Cu(I)-N-graphene	Zn plate	6 M KOH	0.4	Air	~210	S11 ^[16]
NiFeO@MnO _x Core–Shell Structures	Zn plate	6 M KOH	0.25	Air	81	S12 ^[17]
ZnCo ₂ O ₄ /N-CNT	Zn plate	6 M KOH	2.0	Air	82.3	S13 ^[18]
Co ₃ O ₄ nanoparticle supported NGr	Zn foil	6 M KOH	1.0	Air	190	S14 ^[19]
Co(OH) ₂ /N-doped reduced graphene oxide	Zn plate	6 M KOH	1.0	Air	44	S15 ^[20]
3D N-doped CNT arrays	Zn foil	6 M KOH + 0.2 M Zn(Ac) ₂	---	Air	190	S16 ^[21]
Fe-NSCNT	Zn foil	6 M KOH	1.0	Air	100	S17 ^[22]
Litchi-like S-treated Fe/N/C	Zn plate	6 M KOH + 0.2 M Zn(Ac)₂	1.0	Air	~250	This work

Table S3. On-set potential and half-wave potential parameters.

Samples	Potential values	
	On-set potential ^a	Half-wave potential
Untreated Fe/N/C	0.98 V	0.87 V
S-treated Fe/N/C (SPRMs/S=0.5)	0.99 V	0.875 V
S-treated Fe/N/C (SPRMs/S=1)	1.02 V	0.88 V
S-treated Fe/N/C (SPRMs/S=1.5)	1.02 V	0.875 V
Pt/C (20%, E-TEK)	0.92 V	0.81 V

^a(here we define the potential at 0.2 mA cm⁻² as on-set potential)

Reference

- [1] Q. Wei, Y. Fu, G. Zhang, Y. Wang, X. Wang, M. Mohamedi, S. Sun, *RSC Advances* **2016**, 6, 84149.
- [2] M. Lefèvre, E. Proietti, F. Jaouen, J.-P. Dodelet, *science* **2009**, 324, 71.
- [3] E. Proietti, F. Jaouen, M. Lefèvre, N. Larouche, J. Tian, J. Herranz, J.-P. Dodelet, *Nature communications* **2011**, 2, 416.
- [4] G. Zhang, R. Chenitz, M. Lefèvre, S. Sun, J.-P. Dodelet, *Nano Energy* **2016**, 29, 111.
- [5] L. Yang, N. Larouche, R. Chenitz, G. Zhang, M. Lefèvre, J.-P. Dodelet, *Electrochimica Acta* **2015**, 159, 184.
- [6] J. Wang, H. Wu, D. Gao, S. Miao, G. Wang, X. Bao, *Nano Energy* **2015**, 13, 387.
- [7] J. Zhu, M. Xiao, Y. Zhang, Z. Jin, Z. Peng, C. Liu, S. Chen, J. Ge, W. Xing, *ACS Catalysis* **2016**, 6, 6335.
- [8] L. Wang, C. Yang, S. Dou, S. Wang, J. Zhang, X. Gao, J. Ma, Y. Yu, *Electrochimica Acta* **2016**, 219, 592.
- [9] F. Meng, H. Zhong, D. Bao, J. Yan, X. Zhang, *Journal of the American Chemical Society* **2016**, 138, 10226.
- [10] L.-N. Han, L.-B. Lv, Q.-C. Zhu, X. Wei, X.-H. Li, J.-S. Chen, *Journal of Materials Chemistry A* **2016**, 4, 7841.
- [11] B. Wang, X. Wang, J. Zou, Y. Yan, S. Xie, G. Hu, Y. Li, A. Dong, *Nano Letters* **2017**, 17, 2003.
- [12] P. Chen, T. Zhou, L. Xing, K. Xu, Y. Tong, H. Xie, L. Zhang, W. Yan, W. Chu, C. Wu, *Angewandte Chemie International Edition* **2017**, 56, 610.
- [13] X. Han, X. Wu, C. Zhong, Y. Deng, N. Zhao, W. Hu, *Nano Energy* **2017**, 31, 541.
- [14] G. Nam, J. Park, M. Choi, P. Oh, S. Park, M. G. Kim, N. Park, J. Cho, J.-S. Lee, *ACS nano* **2015**, 9, 6493.
- [15] X. Zhang, R. Liu, Y. Zang, G. Liu, G. Wang, Y. Zhang, H. Zhang, H. Zhao, *Chemical Communications* **2016**, 52, 5946.
- [16] H. Wu, H. Li, X. Zhao, Q. Liu, J. Wang, J. Xiao, S. Xie, R. Si, F. Yang, S. Miao, *Energy & Environmental Science* **2016**, 9, 3736.
- [17] Y. Cheng, S. Dou, J.-P. Veder, S. Wang, M. Saunders, S. P. Jiang, *ACS Applied Materials & Interfaces* **2017**, 9, 8121.
- [18] Z. Q. Liu, H. Cheng, N. Li, T. Y. Ma, Y. Z. Su, *Advanced Materials* **2016**, 28, 3777.
- [19] S. K. Singh, V. M. Dhavale, S. Kurungot, *ACS applied materials & interfaces* **2015**, 7, 21138.
- [20] Y. Zhan, G. Du, S. Yang, C. Xu, M. Lu, Z. Liu, J. Y. Lee, **2015**.
- [21] Z. Li, M. Shao, Q. Yang, Y. Tang, M. Wei, D. G. Evans, X. Duan, *Nano Energy* **2017**.
- [22] S. Zeng, F. Lyu, H. Nie, Y. Zhan, H. Bian, Y. Tian, Z. H. E. Li, A. Wang, J. Lu, Y. Y. Li, *Journal of Materials Chemistry A* **2017**.